Intervention in hepatic lipid metabolism : implications for atherosclerosis progression and regression

Li, Z.

Chapter 5

Effects of pyrazole partial agonists on HCA_2-mediated flushing and hepatic VLDL production in mice

Zhaosha Li[1*], Clara C. Blad[2*], Ronald J. van der Sluis[1], Henk de Vries[2], Theo J.C. Van Berkel[1], Ad P. IJzerman[2], Menno Hoekstra[1]

[1]Division of Biopharmaceutics, Leiden/Amsterdam Center for Drug Research, Leiden University, The Netherlands.
[2]Division of Medicinal Chemistry, Leiden/Amsterdam Center for Drug Research, Leiden University, The Netherlands.
[*]These authors contributed equally to this work.

Submitted for publication

ABSTRACT

Background & Aims: Nicotinic acid, also known as niacin, is the most effective agent currently available to treat dyslipidaemic disorders. However, its clinical use has been limited due to the cutaneous flushing, which is mediated by the nicotinic acid receptor HCA_2. In the current study, we assessed the *in vitro* and *in vivo* properties of two partial agonists for HCA_2, LUF6281 and LUF6283, to evaluate their anti-dyslipidemic potentials and cutaneous flushing side effect compared to nicotinic acid.
Methods and Results: Radioligand competitive binding assay showed the K_i values for LUF6281 and LUF6283 were 3 μM and 0.55 μM, respectively. [^{35}S]-GTPγS binding determined the rank order of their potency: nicotinic acid > LUF6283 > LUF6281. Both LUF6281 and LUF6283 avoided the unwanted flushing side effect as tested in C57BL/6 mice. Furthermore, both agonists significantly reduced plasma VLDL-cholesterol concentration in mice. In the liver, both agonists resulted in a more than 40% reduction in the expression levels of ApoB and MTP as compared to the control group, indicating inhibited hepatic VLDL production.
Conclusions: The current study demonstrates that two HCA_2 partial agonists of the pyrazole class are promising drug candidates to achieve the beneficial lipid-lowering effects while successfully avoiding the unwanted flushing side effect.
Keywords: HCA_2 partial agonists, niacin, lipoprotein, VLDL, liver, flushing

INTRODUCTION

Nicotinic acid, also known as niacin, is the most effective agent currently available to treat dyslipidaemic disorders[1]. It lowers plasma levels of pro-atherogenic lipids, including chylomicrons, very-low-density lipoproteins (VLDL), low-density lipoproteins (LDL), and triglycerides (TG) in normolipidemic as well as hypercholesterolemic subjects[2]. Several clinical trials have shown that nicotinic acid reduces cardiovascular disease and myocardial infarction incidence, providing a solid rationale for the use of nicotinic acid in the treatment of atherosclerosis[3,4]. The G protein-coupled receptor GPR109A, also known as PUMA-G in mouse and HM74A in humans, has been identified as a high-affinity receptor for nicotinic acid[5,6]. We now know that the endogenous ligand for GPR109A is 3-hydroxybutyrate, and this receptor has recently been renamed as hydroxy-carboxylic acid receptor 2 (HCA_2)[7].

Despite its established cardiovascular benefits, the clinical use of nicotinic acid has been limited due to the cutaneous flushing, a well-recognized adverse skin effect from nicotinic acid therapy. Flushing has been cited as the major reason for the discontinuation of this therapy, estimated at rates as high as 25%-40%[8]. The nicotinic acid receptor HCA_2 expressed in the skin is a critical mediator of nicotinic acid-induced flushing[9]. Nicotinic acid stimulates HCA_2 in epidermal Langerhans cells and keratinocytes, causing the cells to produce vasodilatory prostaglandin D_2 (PGD_2) and prostaglandin E_2 (PGE_2), which leads to cutaneous vasodilation[10,11,12,13].

For the past decade, the pharmacology of HCA_2 has been studied and full or partial agonists for HCA_2 have been developed in an attempt to achieve the beneficial effects of nicotinic acid while avoiding the unwanted flushing side effect[14]. Based on the structure-activity relationship of nicotinic acid-related molecules, several potent agonists for HCA_2 have been identified, including acipimox, acifran, 3-pyridine-acetic acid, 5-methylnicotinic acid, pyridazine-4-carboxylic acid, and pyrazine-2-carboxylic acid[15,16]. However, the challenge remains that HCA_2 partial agonists failed to demonstrate the beneficial effects on LDL-cholesterol, triglycerides or HDL-cholesterol despite the absence of flushing events in clinical studies[17]. Further understanding of the medicinal chemistry of HCA_2 is needed to pharmacologically dissociate the antilipolytic and vasodilatory effects of nicotinic acid by acting on HCA_2[16].

In the current study, we assessed the properties of two HCA_2 partial agonists, LUF6281 and LUF6283, of the pyrazole class, which were developed in our laboratory[18]. We first characterized these two compounds *in vitro*, using a radioligand binding assay, [^{35}S]-GTPγS assay and ERK phosphorylation assay. The ERK phosphorylation assay was included because it has been suggested that ERK1/2 phosphorylation downstream from HCA_2 correllates positively with skin flushing[19]. Then, we assessed the cutaneous flushing effect and the therapeutic lipid-lowering potential of these two partial agonists in C57BL/6 mice.

MATERIALS AND METHODS

In vitro experiments

Materials

[^{3}H]-nicotinic acid (60 Ci/mmol) was obtained from BioTrend (Koehln, Germany). [^{35}S]-GTPγS (1250 Ci/mmol) was obtained from Perkin Elmer (Waltham, MA).

Cell culture and membrane preparation

Human embryonic kidney (HEK) 293T cells stably expressing human HCA_2 were cultured in DMEM supplemented with 10% newborn bovine serum, 0.4 mg/mL G418, 50 IU/mL penicillin and 50 µg/mL streptomycin. The cells were harvested by scraping in cold PBS, centrifuged at 1000 xg for 10 minutes and resuspended in cold 50 mM Tris-HCl buffer, pH 7.4. Then a DIAX 900 electrical homogenizer (Heidolph, Schwabach, Germany) was used for 15 seconds to obtain cell lysis. The suspension was centrifuged at 225000 xg for 20 minutes at 4 °C and the supernatant was discarded. The pellet was resuspended in Tris-HCl, and the homogenization and centrifugation steps were repeated. The membranes were resuspended in cold assay buffer (50 mM Tris HCl, 1 mM $MgCl_2$, pH 7.4) and the protein content was determined using BCA assay (Thermo Scientific, Waltham, USA). During membrane preparation the suspension was kept on ice at all times. Membrane aliquots were stored at -80 °C until the day of use.

[^{3}H]-nicotinic acid displacement assay

Membranes of our stable HEK293T-HCA_2 cell line (50 µg protein per tube) were incubated for 1 hour at 25 °C with 20 nM [^{3}H]-nicotinic acid and with increasing concentrations of the test compounds in assay buffer (50 mM Tris HCl, 1 mM $MgCl_2$, pH 7.4). The total assay volume was 100 µL. To assess the total binding, a control without test compound was included. The non-specific binding was determined in the presence of 10 µM unlabeled nicotinic acid. Final DMSO concentration in all samples was ≤ 0.25%. The incubation was terminated by filtering over GF/B filters using a 24-sample harvester (Brandel, Gaithersburg, USA). The filters were washed 3 times with 2 mL cold buffer (50 mM Tris HCl, pH 7.4). Filters were transferred to counting vials and counted in a Perkin Elmer LSA Tri-Carb 2900TR counter after 2 hours of extraction in 3.5 mL Emulsifier Safe liquid scintillation cocktail (Perkin Elmer, Waltham, USA).

[^{35}S]-GTPγS binding assay

This assay was performed in 96-well format in 50 mM Tris-HCl, 1 mM EDTA, 5 mM $MgCl_2$, 150 mM NaCl, pH 7.4 at 25 °C with 1 mM DTT, 0.5% BSA and 50 µg/mL saponin freshly added. HEK-HCA_2 membranes (5 µg protein per well in 25 µL) were pre-incubated with 25 µL of 40 µM GDP and 25 µL increasing concentrations of the test compounds, for 30 minutes at room temperature. Then, 25 µL [^{35}S]-GTPγS was added (final concentration 0.3 nM) and the mixture was incubated for 90 minutes at 25 °C with constant shaking. The incubation was terminated by filtration over GF/B filterplates on a FilterMate harvester (PerkinElmer). The filters were dried and 25 µL Microscint 20 (PerkinElmer) was added to each filter. After ≥3 hours of extraction the bound radioactivity was determined in a Wallac Microbeta Trilux 1450 counter (PerkinElmer, MA, USA).

ERK1/2 phosphorylation assay
The assay was performed using AlphaScreen SureFire Phospho-ERK1/2 kit (PerkinElmer, MA, USA), following the kit protocol. Briefly, a 96-well cell culture plate was coated with poly-D-lysine and HEK cells stably expressing human HCA_2 were seeded at 50000 cells/well in 200 µL DMEM supplemented with 10% newborn bovine serum, 0.4 mg/mL G418, 50 IU/mL penicillin and 50 µg/mL streptomycin. After overnight incubation the cells were serum starved for 4 h in the same medium lacking the serum, and then the medium was replaced by 90 µL prewarmed PBS and incubated for an additional 30 minutes. Increasing concentrations of the test compounds were diluted in prewarmed PBS and 10 µL was added per well for stimulation. After 5 minutes the stimulation solution was removed from the plates, the wells were washed once in ice-cold PBS and 100 µL lysis buffer was added per well. After 15 minutes of incubation and shaking at room temperature, the lysates were mixed by pipetting and 4 µL was transferred to a 384-well OptiPlate (PerkinElmer, MA, USA). The reaction mix was prepared according to the kit protocol (60 µL reaction buffer and 10 µL activation buffer with 1 µL of the donor and acceptor beads each) and 7 µL mix was added to each proxyplate well. After 2 h the plate was read on an EnVision multilabel plate reader (PerkinElmer, MA, USA).

Data analysis
Analysis of the results was performed using Prism 5.0 software (GraphPad Software Inc., La Jolla, USA). Nonlinear regression was used to determine IC_{50} values from competition binding curves. The Cheng-Prusoff equation was then applied to calculate K_i values[20]. [^{35}S]-GTPγS and pERK curves were analysed by nonlinear regression to obtain EC_{50} values.

***In vivo* experiments**

Animals
Female C57BL/6 mice of 12 weeks old were used. Animals were fed a regular cholesterol-free chow diet containing 4.3% (w/w) fat (RM3, Special Diet Services, Witham, UK). Mice received either vehicle (50% DMSO in PBS) or HCA_2 partial agonists LUF6281 and LUF6283 (400 mg/kg/day) once a day for 4 weeks via oral gavage. After euthanization, mice were bled via orbital exsanguination and perfused *in situ* through the left cardiac ventricle with ice-cold PBS (pH 7.4) for 20 minutes. Liver was dissected free of fat and snap-frozen in liquid nitrogen. Animal care and procedures were performed in accordance with the national guidelines for animal experimentation. All protocols were approved by the Ethics Committee for Animal Experiments of Leiden University.

Measurement of skin flushing in mouse
Cutaneous flushing in C57BL/6 mice was assessed by monitoring the change of the skin temperature at the mouse paw location. Temperature measurements were recorded using a non contact infrared thermometer (Pro Exotics PE-1 Infrared Temp Gun, Littleton, USA). The probe was held at a distance of 1 to 2 mm from the metacarpal pad of mouse paw, and temperature readings were taken from a circular area approximately 3 mm in diameter. Animals were habituated to handling and to the infrared probe before use. Skin temperature was initially recorded from

the abdominal area, tail, ear, and paw, after which it was determined that mouse paw skin temperature gave the most reliable and consistent results. During the experiment, the animals were dosed with either vehicle (50% DMSO in PBS) or partial agonists LUF6281 and LUF6283 (400 mg/kg/day) via oral gavage (10:00-11:00 AM), and the paw temperature was measured every 10 minutes for a period of 60 minutes in total. Three readings from the center area of mouse paw were recorded routinely for each time point. Baseline paw temperature was recorded right before animals were dosed. All the administration was performed in conscious mice to avoid the interference of the anesthetics on skin temperature.

Plasma lipid analysis

The distribution of cholesterol over different lipoproteins in plasma was determined by fast protein liquid chromatography (FPLC) through a Superose 6 column (3.2 x 30 mm; Smart-System, Pharmacia, Uppsala, Sweden). Cholesterol content of the lipoprotein fractions was measured using the enzymatic colorimetric assay (Roche Diagnostics, Mannheim, Germany).

RNA isolation and gene expression analysis.

Total RNA from the liver was isolated using acid guanidinium thiocyanate (GTC)-phenol-chloroform extraction. Briefly, 500 µL of GTC solution (4 M guanidine isothiocyanate, 25 mM sodium citrate, 0.5% N-lauroylsarcosine) was added to each sample, followed by acid phenol:chloroform extraction. The RNA in aqueous phase was precipitated with isopropanol. The quantity and purity of the isolated RNA were examined using ND-1000 Spectrophotometer (Nanodrop, Wilmington, DE, USA). One microgram of the isolated RNA from each sample was converted into cDNA by reverse transcription with RevertAid™ M-MuLV Reverse Transcriptase (Promega, Madison, WI, USA). Negative controls without addition of reverse transcriptase were prepared for each sample. Quantitative real-time PCR was carried out using ABI Prism 7700 Sequence Detection system (Applied Biosystems, Foster City, CA, USA) according to the manufacturer's instructions. 36B4, Beta-actin, and GAPDH were used as internal housekeeping genes. The gene-specific primer sequences used are listed in Table 1. Amplification curves were analyzed using 7500 Fast System SDS software V1.4 (Applied Biosystems, Foster City, CA, USA). The relative expression of each gene was expressed as fold changes $2^{-(\Delta\Delta CT)}$ compared to baseline group. Standard error of the mean (SEM) and statistical significance were calculated using ΔΔCt formula.

Statistical analysis

Mean values between 2 groups were analyzed with 2-tailed unpaired Student's t-test. Data sets containing multiple groups were analyzed by ANOVA (Instat GraphPad software, San Diego, USA). Statistical significance was defined as $p<0.05$. Data are expressed as means ± SEM.

Table 1. Murine primers for quantitative real-time PCR analysis

Gene	Forward primer	Reverse Primer
36B4	GGACCCGAGAAGACCTCCTT	GCACATCACTCAGAATTTCAATGG
Beta-actin	AACCGTGAAAAGATGACCCAGAT	CACAGCCTGGATGGCTACGTA
GAPDH	TCCATGACAACTTTGGCATTG	TCACGCCACAGCTTTCCA
ApoB	ATGTCATAATTGCCATAGATAGTGCCA	TCGCGTATGTCTCAAGTTGAGAG
MTP	AGCTTTGTCACCGCTGTGC	TCCTGCTATGGTTTGTTGGAAGT

RESULTS

In this study, we assessed the *in vitro* and *in vivo* properties of two HCA_2 ligands, LUF6281 and LUF6283, to evaluate their anti-dyslipidemic potentials and cutaneous flushing side effect compared to nicotinic acid. The chemical structures of these compounds are shown in Figure 1. For *in vitro* experiments we used HEK293T cell line stably expressing the human HCA_2 receptor.

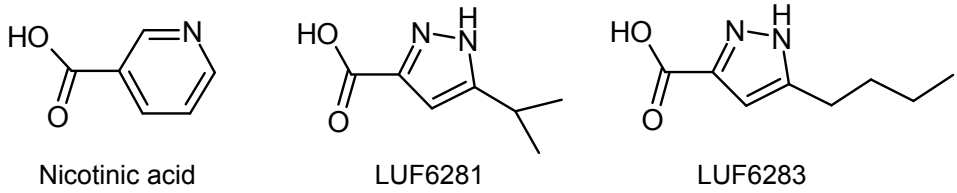

Nicotinic acid LUF6281 LUF6283

Figure 1. Chemical structures of nicotinic acid, LUF6281, and LUF6283.

First, the affinity of the compounds to HCA_2 was determined by a competitive binding assay using radiolabeled nicotinic acid (Figure 2). The K_i values determined for LUF6281 and LUF6283 were 3 μM and 0.55 μM, respectively (Table 2).

Next, we compared the potencies and intrinsic efficacies of nicotinic acid, LUF6281 and LUF6283 by measuring their ability to stimulate [^{35}S]-GTPγS binding. The results clearly showed that LUF6281 and LUF6283 were partial agonists, with intrinsic efficacies of 55 (±4.1) and 76 (±3.4) %, respectively (N=7). The rank order of their potency was nicotinic acid > LUF6283 > LUF6281, with EC_{50} values of 0.41, 3.1 and 8.6 μM, respectively (Figure 3; Table 2).

Table 2. In vitro biochemical characterization of GPR109A agonists nicotinic acid, LUF6281, and LUF6283. Values are mean (±SEM) (N≥3)

	Ki (μM)	**EC_{50}-[^{35}S]-GTPγS (μM)**	**EC_{50}-pERK1/2 (μM)**
Nicotinic acid	0.04 (±0.02)	0.41 (±0.11)	0.02 (±0.004)
LUF6281	3.1 (±0.5)	8.60 (±1.00)	1.37 (±0.31)
LUF6283	0.55 (±0.01)	3.10 (±0.13)	0.32 (±0.06)

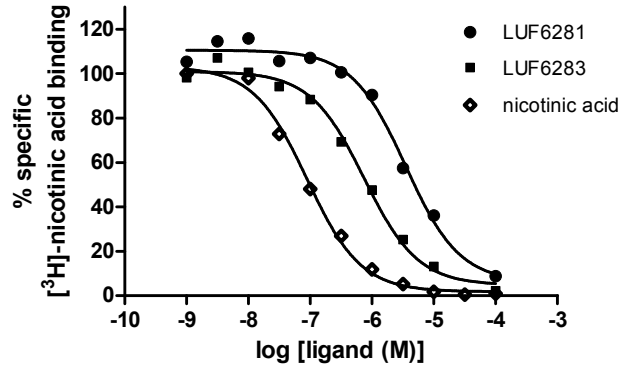

Figure 2. Competitive radioligand binding assay using 20 nM [^{3}H]-nicotinic acid revealing the relative affinities of nicotinic acid, LUF6481 and LUF6483. The assay was performed on HEK293T-HCA_2 membranes (50 µg/tube). The results from one representative experiment are shown (of N=3).

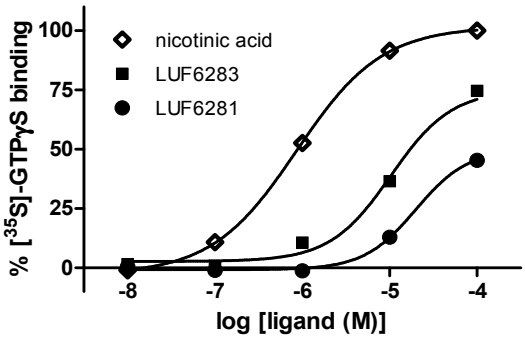

Figure 3. Dose-response curves of nicotinic acid, LUF6481 and LUF6483 in a [^{35}S]-GTPγS binding assay, showing the relative potencies and intrinsic efficacies. Nicotinic acid is a full agonist, whereas LUF6481 and LUF6483 are partial agonists in this assay. The assay was performed on HEK293T-HCA_2 membranes (5 µg/tube). Data from one representative experiment are shown (of N=3).

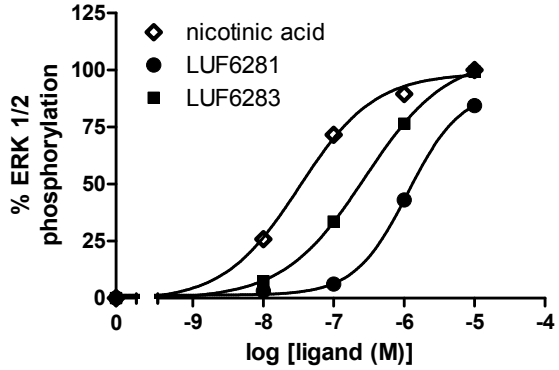

Figure 4. Dose-response curves of nicotinic acid, LUF6481 and LUF6483 in an ERK 1/2 phosphorylation assay, showing the relative potencies and intrinsic efficacies. All ligands are full agonists in this assay. The assay was performed on attached HEK293T-HCA_2 cells. Data from one representative experiment are shown (of N=3-5).

The second functional assay monitored ERK1/2 phosphorylation of the compounds upon HCA_2 activation. Results from this assay showed that the intrinsic efficacy was the same for all compounds (Figure 4; Table 2). The EC_{50} values obtained here were 20 nM for nicotinic acid, 1.6 µM for LUF6281 and 0.26 µM for LUF6283. Thus, all compounds seemed to be more potent in the pERK1/2 assay than in the [^{35}S]-GTPγS assay, but this difference was much more pronounced for nicotinic acid (20-fold) than for LUF6283 (12-fold) and LUF6281 (4-fold) (Table 2).

To examine the vasodilatory effects of these compounds *in vivo*, we used C57BL/6 mice to assess the cutaneous flushing as determined by an increase in mouse paw skin temperature. In mice, the normal paw skin temperature was approximately 26.4°C (*n* = 30). Mice were divided into 3 groups: the control group received vehicle (50% DMSO in PBS), while the treatment groups received LUF6281 and LUF6283 (400 mg/kg/day) respectively via oral gavage. Surprisingly, DMSO induced a time-dependent temperature increase in the control group, with a maximum 3.6 °C (*n* = 10) that occurred at 20 minutes after oral gavage (Figure 5). Similar effects of DMSO have been reported in the literature, and might be due to a release of histamine[21,22,23,24,25]. However, neither of the treatment groups displayed significant temperature raise. At 20 minutes, LUF6281 and LUF6283 induced a maximal temperature increase of only 0.5 or 1.0 °C (*n* = 10 per group), which was significantly lower than the temperature raise observed in the control group ($p < 0.001$; Figure 5) and comparable to the temperature raise induced by PBS at the same time point (data not shown). The results suggested that both of the HCA_2 partial agonists LUF6281 and LUF6283 avoided the unwanted flushing side effect in mice.

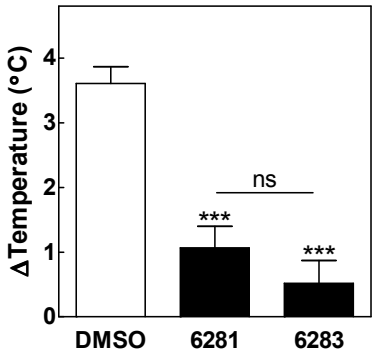

Figure 5. Mouse flushing after administration of nicotinic acid, LUF6281, and LUF6283. The cutaneous vasodilation was determined by change in paw skin temperature in C57BL/6 mice. Mice received vehicle (DMSO), LUF6281, or LUF6283 (400 mg/kg/day) via oral gavage. Data are expressed as the increase of skin temperature at 20 min after dosing compared to before treatment (n=10 per group). ns, not significant. ***P<0.001.

To evaluate the beneficial antilipolytic potentials of the LUF compounds, we tested their effects on plasma lipid homeostasis in C57BL/6 mice. Although treatment with LUF compounds for 4 weeks did not alter plasma total cholesterol or triglycerides concentration, separation of plasma lipoproteins by FPLC in combination with analysis of the lipid content across the FPLC fractions showed that LUF6281 sharply reduced plasma VLDL-cholesterol concentration by 77.4% ($p<0.01$) and LUF6283 also significantly reduced plasma VLDL-cholesterol level by 38.1% ($p<0.05$, Figure 6).

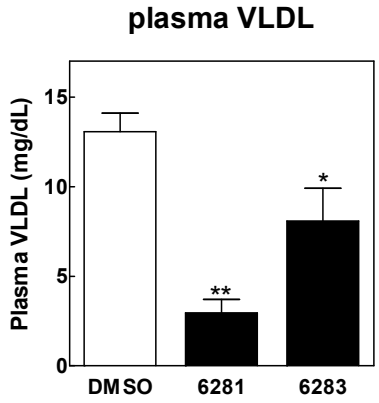

Figure 6. Effects of LUF6281 and LUF6283 on plasma VLDL concentration in C57BL/6 mice. Mice were fed with regular chow diet and received either vehicle (DMSO) or GPR109A partial agonists LUF6281 and LUF6283 (400 mg/kg/day) once a day for 4 weeks. Plasma lipoproteins were separated by FPLC and cholesterol level was measured in each fraction. VLDL represents the sum of cholesterol concentrations from fraction 2 to 7 (VLDL fractions. Values are means ± SEM (n=10 per group). *P<0.05; **P<0.01.

To further understand the mechanism whereby LUF compounds largely reduced the plasma VLDL concentration, hepatic gene expression levels in response to compound treatment were assessed by real-time quantitative PCR. Both LUF6281 and LUF6283 modulated the relative RNA expression level of hepatic VLDL production-associated genes in mouse. Concomitant with the plasma VLDL-lowering effect, treatment of both LUF compounds resulted in a more than 40% reduction in the expression levels of apolipoprotein B (apoB) ($p<0.05$) and microsomal triglyceride transfer protein (MTP) ($p<0.05$) as compared to the control group (Figure 7), indicating inhibited hepatic VLDL production.

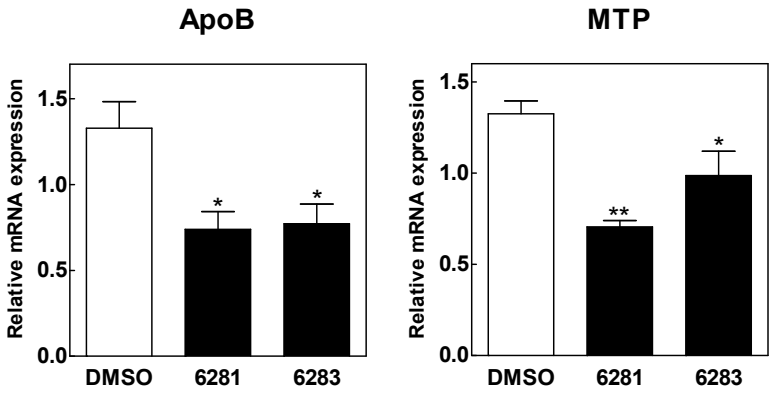

Figure 7. Effects of LUF6281 and LUF6283 on hepatic gene expression in C57BL/6 mice. Total RNA was extracted from liver, and relative mRNA expression levels of ApoB and MTP were determined by quantitative PCR and presented as fold-change relative to control group. Values are means ± SEM (n=10 per group). *P<0.05; **P<0.01.

DISCUSSION

Previous studies have shown that HCA_2 mediates nicotinic acid-induced cutaneous flushing[26]. It seems that the early phase of flushing depends on HCA_2 expressed on Langerhans cells, whereas the late phase is mediated by HCA_2 expressed on keratinocytes[12]. Derivatives of nicotinic acid have been developed to pharmacologically dissociate the antilipolytic and vasodilatory effects by acting as partial and, in the case of MK-0354, biased agonists on HCA_2[18,19,27]. The pyrazole MK-0354 stimulates the G protein pathway that leads to antilipolysis in adipocytes, but does not cause ERK1/2 phosphorylation[27]. This compound showed promising results in mice, since no vasodilation was observed and antilipolytic activity was retained, but in clinical trials this compound failed since it had no effect on plasma lipid levels[17]. In the current study, we characterized the affinity and efficacy of two HCA_2 partial agonists LUF6281 and LUF6283 previously reported by us[18] and we evaluated the cutaneous flushing effect and the therapeutic lipid-lowering potential of these agonists in C57BL/6 mice.

We show that nicotinic acid, LUF6281 and LUF6283 may all have a certain bias, since these compounds all seem to have a higher potency for ERK1/2 phosphorylation than for G protein activation. Furthermore, LUF6281 and LUF6283 were both partial agonists in the [^{35}S]-GTPγS assay but seemed full agonists in the pERK1/2 assay. The fold difference in potency depended on the compound; nicotinic acid was 20-fold more potent for ERK phosphorylation, LUF6283 was 12-fold more potent and LUF6281 was only 5-fold more potent. The high potency of nicotinic acid for activation of the MAP kinase pathway may explain why this compound causes flushing so effectively. Unlike MK-0354, our pyrazole compounds are still active in the ERK1/2 assay, but we hypothetized that their relatively low potency on this pathway might attenuate the flushing response. Indeed, our *in vivo* findings confirm that the pyrazoles do not provoke the flushing response as nicotinic acid does, although it remains unclear what causes this improvement.

In addition, our data suggested that LUF6281 and LUF6283 exerts lipid-lowering effect via inhibiting hepatic VLDL production. LUF6281 and LUF6283 both markedly reduced the hepatic gene expression of apoB and MTP. ApoB is the structural lipoprotein of VLDL, LDL and chylomicrons. ApoB and the MTP are essential for the assembly and secretion of apoB-containing lipoproteins[28]. The assembly and secretion pathway of VLDL in the liver involves the transfer of lipid by MTP to apoB during translation and then the fusion of apoB-containing precursor particles with triglyceride droplets to form mature VLDL[29,30]. The link between hepatic ApoB / MTP gene expression level, hepatic VLDL secretion and plasma VLDL concentration has been illustrated in the literature[31,32].

In conclusion, the current study demonstrated two HCA_2 partial agonists of the pyrazole class as promising drug candidates to achieve the beneficial lipid-lowering effects while successfully avoid the unwanted flushing side effect.

ACKNOWLEDGEMENTS

This work was supported by TIPharma (Grant D1-105 to C.C.B., A.P.IJ.; Grant T2-

110 to Z.L., T.J.C.V.B., M.H.) and the Netherlands Heart Foundation (Grant 2008T070 to M.H.).

REFERENCES

1. Benhalima, K. and E. Muls, Niacin, an old drug with new perspectives for the management of dyslipidaemia. Acta Clin Belg, 2010. 65(1): p. 23-8.
2. Carlson, L.A., Niaspan, the prolonged release preparation of nicotinic acid (niacin), the broad-spectrum lipid drug. Int J Clin Pract, 2004. 58(7): p. 706-13.
3. Lee, J.M., et al., Effects of high-dose modified-release nicotinic acid on atherosclerosis and vascular function: a randomized, placebo-controlled, magnetic resonance imaging study. J Am Coll Cardiol, 2009. 54(19): p. 1787-94.
4. Taylor, A.J., et al., Extended-release niacin or ezetimibe and carotid intima-media thickness. N Engl J Med, 2009. 361(22): p. 2113-22.
5. Lorenzen, A., et al., Characterization of a G protein-coupled receptor for nicotinic acid. Mol Pharmacol, 2001. 59(2): p. 349-57.
6. Wise, A., et al., Molecular identification of high and low affinity receptors for nicotinic acid. J Biol Chem, 2003. 278(11): p. 9869-74.
7. Offermanns, S., et al., International Union of Basic and Clinical Pharmacology. LXXXII: Nomenclature and Classification of Hydroxy-carboxylic Acid Receptors (GPR81, GPR109A, and GPR109B). Pharmacol Rev, 2011. 63(2): p. 269-90.
8. Davidson, M.H., Niacin use and cutaneous flushing: mechanisms and strategies for prevention. Am J Cardiol, 2008. 101(8A): p. 14B-19B.
9. Benyó, Z., et al., GPR109A (PUMA-G/HM74A) mediates nicotinic acid-induced flushing. J Clin Invest, 2005. 115(12): p. 3634-3640.
10. Cheng, K., et al., Antagonism of the prostaglandin D2 receptor 1 suppresses nicotinic acid-induced vasodilation in mice and humans. Proc Natl Acad Sci U S A, 2006. 103(17): p. 6682-7.
11. Dunbar, R.L. and J.M. Gelfand, Seeing red: flushing out instigators of niacin-associated skin toxicity. J Clin Invest, 2010. 120(8): p. 2651-5.
12. Hanson, J., et al., Nicotinic acid- and monomethyl fumarate-induced flushing involves GPR109A expressed by keratinocytes and COX-2-dependent prostanoid formation in mice. J Clin Invest, 2010. 120(8): p. 2910-9.
13. Morrow, J.D., et al., Identification of skin as a major site of prostaglandin D2 release following oral administration of niacin in humans. J Invest Dermatol, 1992. 98(5): p. 812-5.
14. Wanders, D. and R.L. Judd, Future of GPR109A agonists in the treatment of dyslipidemia. Diabetes Obes Metab, 2011.
15. Kamanna, V.S. and M.L. Kashyap, Nicotinic acid (niacin) receptor agonists: Will they be useful therapeutic agents? Am J Cardiol, 2007. 100(11): p. 53N-61N.
16. Soudijn, W., I. van Wijngaarden, and A.P. IJzerman, Nicotinic acid receptor subtypes and their ligands. Med Res Rev, 2007. 27(3): p. 417-433.
17. Lai, E., et al., Effects of a niacin receptor partial agonist, MK-0354, on plasma free fatty acids, lipids, and cutaneous flushing in humans. J Clin Lipidol, 2008. 2(5): p. 375-83.
18. van Herk, T., et al., Pyrazole derivatives as partial agonists for the nicotinic acid receptor. J Med Chem, 2003. 46(18): p. 3945-51.
19. Richman, J.G., et al., Nicotinic acid receptor agonists differentially activate downstream effectors. J Biol Chem, 2007. 282(25): p. 18028-18036.
20. Cheng, Y. and W.H. Prusoff, Relationship between the inhibition constant (K1) and the concentration of inhibitor which causes 50 per cent inhibition (I50) of an enzymatic reaction. Biochem Pharmacol, 1973. 22(23): p. 3099-108.
21. Adamson, J.E., H.H. Crawford, and C.E. Horton, The action of dimethyl sulfoxide on the experimental pedicle flap. Surg Forum, 1966. 17: p. 491-2.
22. Colucci, M., et al., New insights of dimethyl sulphoxide effects (DMSO) on experimental in vivo models of nociception and inflammation. Pharmacol Res, 2008. 57(6): p. 419-25.
23. Jacob, S.W. and R. Herschler, Pharmacology of DMSO. Cryobiology, 1986. 23(1): p. 14-27.
24. Kligman, A.M., Topical Pharmacology and Toxicology of Dimethyl Sulfoxide. 1. JAMA, 1965. 193: p. 796-804.
25. Santos, N.C., et al., Multidisciplinary utilization of dimethyl sulfoxide: pharmacological, cellular, and molecular aspects. Biochem Pharmacol, 2003. 65(7): p. 1035-41.
26. Zhang, Y.Y., et al., Niacin mediates lipolysis in adipose tissue through its G protein-coupled receptor HM74A. Biochem Biophys Res Commun, 2005. 334(2): p. 729-732.
27. Semple, G., et al., 3-(1H-tetrazol-5-yl)-1,4,5,6-tetrahydro-cyclopentapyrazole (MK-0354): A partial agonist of the nicotinic acid receptor, G protein-coupled receptor 109A, with antilipolytic but no vasodilatory activity in mice. J Med Chem, 2008. 51(16): p. 5101-5108.

28. Davidson, N.O. and G.S. Shelness, APOLIPOPROTEIN B: mRNA editing, lipoprotein assembly, and presecretory degradation. Annu Rev Nutr, 2000. 20: p. 169-93.
29. Davis, R.A., Cell and molecular biology of the assembly and secretion of apolipoprotein B-containing lipoproteins by the liver. Biochim Biophys Acta, 1999. 1440(1): p. 1-31.
30. Shelness, G.S. and J.A. Sellers, Very-low-density lipoprotein assembly and secretion. Curr Opin Lipidol, 2001. 12(2): p. 151-7.
31. Bartolomé, N., et al., Kupffer cell products and interleukin 1beta directly promote VLDL secretion and apoB mRNA up-regulation in rodent hepatocytes. Innate Immun, 2008. 14(4): p. 255-66.
32. Basciano, H., et al., LXRalpha activation perturbs hepatic insulin signaling and stimulates production of apolipoprotein B-containing lipoproteins. Am J Physiol Gastrointest Liver Physiol, 2009. 297(2): p. G323-32.